



Intercomparison of nighttime aerosol optical depth retrievals from both reflectance-based and city light-based methods using VIIRS DNB data

Aanan H. Schlief¹, Jared W. Marquis¹, Jianglong Zhang¹, Jeffrey S. Reid², and Steve Miller³

5 ¹Department of Atmospheric Sciences, University of North Dakota, Grand Forks, ND 58202, USA

²Marine Meteorology Division, US Naval Research Laboratory, Monterey, CA 93943, USA

³Cooperative Institute for Research in the Atmosphere, Colorado State University, Fort Collins, CO 80521, USA

Correspondence to: Jianglong Zhang (jianglong.zhang@und.edu) & Aanan Schlief (aanan.schlief@und.edu)

Abstract.

10 Using observations from the Visible Infrared Imaging Radiometer Suite (VIIRS) Day/Night Band (DNB), two different nighttime aerosol optical depth (AOD) retrieval methods were evaluated and inter-compared. The first approach is a lunar reflectance-based retrieval method, using reflected moonlight in a manner similar to daytime retrievals. The second approach utilizes changes in light patterns over regions with artificial light sources due to the upward diffusion of light by aerosol particles. Both retrieval methods were implemented over Dakar, Senegal for 2017 and 2018. Retrievals from both approaches were evaluated against ground-based solar and lunar AEROSOL ROBOTIC NETWORK (AERONET) data, as well as daytime AOD retrievals from the Moderate Resolution Imaging Spectroradiometer (MODIS). Additionally, impacts of using the Miller and Turner lunar model for estimating Top-Of-Atmosphere (TOA) lunar spectral flux for AOD retrievals were also studied. Findings suggest that while both retrieval methods show skill in retrieving nighttime AOD by qualitatively identifying over-ocean aerosol plume locations and quantitatively comparing with solar and lunar retrieved AERONET data, 15 cloud contamination and variations in lunar properties are factors that need to be carefully quantified in future studies for accurate nighttime aerosol retrievals using VIIRS DNB data. This study suggests that there are sampling issues from both approaches, but the combined use of both retrieval methods can increase the sampling rate for nighttime aerosol retrievals by more than 50%. 20

1 Introduction

25 In passive-based aerosol retrievals, aerosol properties are typically derived during daytime hours from observed top-of-atmosphere reflected solar light (Remer et al., 2005). The lack of solar light during the nighttime makes the retrieval of nighttime aerosol properties using traditional sensors such as from the Moderate Resolution Imaging Spectroradiometer (MODIS) and Multi-angle Imaging SpectroRadiometer (MISR) impossible (e.g. Zhang et al., 2025). However, included in



the Visible Infrared Imaging Radiometer Suite (VIIRS) sensor on-board Suomi-NPP, and the Joint Polar Satellite System (JPSS) series is a calibrated high gain Day/Night Band (DNB) that is able to sense visible lights at levels that can be 10 million times weaker than sunlight (Miller et al., 2013). Using observations from VIIRS DNB, pioneering nighttime aerosol retrieval efforts have been attempted using either 1) reflected moonlight rather than sunlight (e.g. Zhou et al., 2021), or 2) direct light emission brightness from artificial light sources (e.g. Zhang et al., 2008; Johnson et al., 2013) or 3) contrast reduction (variance) over artificial light sources (e.g. McHardy et al., 2015; Zhang et al., 2025).

Related to the more traditional passive retrieval approach, reflected moonlight, which contains information about surface and atmospheric properties (e.g., aerosols), can be applied for retrieving nighttime aerosol properties using a daytime-like approach. In fact, if reflectance is used, which is the measured Top-Of-Atmosphere (TOA) upward radiance from VIIRS DNB normalized by TOA downward lunar flux, single channel daytime AOD retrieval methods may be applicable to nighttime aerosol retrievals. Since reflectance is normalized by TOA downward flux, the observed reflectance from VIIRS DNB shall be similar given the same surface and atmospheric conditions, as well as the same viewing geometries regardless of TOA downward flux magnitude from solar light or moonlight. For example, Zhou et al., (2021) attempted nighttime aerosol retrievals using reflected lunar light over dark surfaces over rural areas in the United States. The study went on to note that the VIIRS DNB lunar reflectance-based retrieval algorithm can be used as a method to provide diurnal aerosol retrievals with the ability to track nighttime aerosols (Zhou et al., 2021).

The lunar reflectance method requires the presence of reflected moonlight, which can't be applicable to nights that lack moonlight such as new moon nights (e.g. Zhang et al., 2025). It is also very challenging to apply the reflected moonlight-based aerosol retrieval method over bright surfaces, where the TOA reflected moonlight is less-sensitive/insensitive to changes in the underneath aerosol layers. Indeed, over land surface albedos are generally enhanced at red wavelengths further reducing contrast as does the potential of residual light emissions. As an alternative method, using nighttime observations from the Defense Meteorological Satellite Program (DMSP) Operational Linescan System (OLS), Zhang et al., (2008) proposed a method of retrieving aerosol optical depth (AOD) using observations over regions with the distribution of artificial light contrasts. The initial hypothesis of the study was that for aerosol polluted cloud free nights, radiance values over artificial light sources, as measured by the DNB, can be much reduced in comparison with aerosol free



and cloud free nights, depending on AOD. McHardy et al., (2015) proposed a revised method for deriving nighttime AODs
55 using variances in radiances (that is reduced sharpness) within an artificial light source known as the *variance method*. The
advantage of the variance method is that only the VIIRS DNB radiance distribution over artificial light sources is needed,
excluding the need for observations from artificial light free regions. This variance method has the additional benefit that the
impact of moonlight on AOD retrievals is much reduced. Following similar methods proposed in McHardy et al., (2015),
Zhang et al., (2019; 2025) extended the study on a much larger spatial and temporal domain demonstrating the possibility of
60 conducting nighttime AOD retrievals using VIIRS DNB data on both local and global scales. While the findings in Zhang et
al., (2019; 2025) were encouraging for the development of an operational nighttime AOD product, misclassification of high
aerosol loading as cloud as well as differences in surface reflectance due to snow still provide complications.

In fact, both the reflected-moonlight based and artificial-light based variance methods are ultimately complimentary
given differences in lower boundary conditions and the availability of lunar and artificial light sources. It is a natural desire
65 to combine both methods for maximum data coverage in space and time. Yet, each method has its strengths and weaknesses
that need to be studied before retrievals from both methods can be properly integrated. It is worth noting that although
pioneer efforts have been conducted for attempting nighttime AOD retrievals based on either reflected moonlight or
attenuated artificial lights, there has yet to be a pairwise comparison of AOD retrievals from both methods. In this study,
using VIIRS DNB observations over the Atlantic Ocean near Dakar, Senegal, AOD retrievals from both methods were
70 attempted and inter-compared for two years of data: 2017 and 2018. The Dakar, Senegal region was selected as this region is
frequently polluted by dust aerosols originating from North Africa. Limitations and caveats of each method, including data
sampling rates and major uncertainty sources, were explored in this study. In addition, the impact of lunar reflectance models
on AOD retrievals, including the use of Miller and Turner model (Miller and Turner, 2009) which estimate TOA
downwelling spectral lunar fluxes needed to approximate VIIRS DNB reflectance, were also studied. Finally, we explored
75 the feasibility of applying a single channel daytime solar reflectance-based method, designed for daytime AOD retrievals
using measured TOA reflected solar light (in unit of reflectance), for lunar AOD retrievals using reflected moonlight (in the
unit of reflectance) by replacing TOA downwelling solar spectral irradiance with lunar spectral irradiance.



2 Datasets and Models

VIIRS DNB data were used for retrieving nighttime aerosol optical depth. MODIS and ground-based AEROSOL
80 RObotic NETwork (AERONET) data were used for evaluating/validating VIIRS nighttime AOD retrievals for the years
2017 and 2018. Details of each dataset are listed below.

2.1 VIIRS DNB Data

The VIIRS sensor onboard the Suomi National Polar-Orbiting Partnership (NPP) satellite includes a Day/Night
Band that is capable of providing passive-based observations of low light scenes at nighttime. The VIIRS DNB is a
85 panchromatic sensor observing at a wavelength range of 0.5-0.9 μm centered at 0.7 μm (Miller et al., 2013; Zhang et al.,
2019). The spatial resolution is ~ 750 m at nadir with a swath width of approximately 3060 km. The VIIRS data for this study
were obtained from the NOAA Comprehensive Large Array-Data Stewardship System (NOAA CLASS;
<https://www.avl.class.noaa.gov/saa/products/>, last access: Apr 16, 2026).

Both VIIRS Environmental Data Records (EDR) and VIIRS Sensor Data Records (SDR) datasets were used in this
90 study. The VIIRS SDR dataset contains VIIRS DNB Geographical Sensor data record (GDNBO) and VIIRS DNB radiance
sensor data (SVDNB) providing DNB radiance and geolocation data. Furthermore, the VIIRS EDR dataset includes VIIRS
DNB cloud cover (VCCLO) and VIIRS cloud-aggregated environmental ellipsoid geolocation (GCDLO) layers data that
were used for cloud screening. Since the VIIRS SVDNB radiance data and cloud products (VCCLO and GCDLO) are
available at different spatial resolutions, VIIRS cloud products were resampled to the spatial resolution of the VIIRS
95 SVDNB data and before being used to cloud screen the VIIRS DNB radiance data (e.g., Zhang et al., 2019; 2025).

2.2 Aqua MODIS Data

The Aqua MODIS daytime aerosol retrievals were used for cross-comparison of nighttime aerosol retrievals from
VIIRS in this study. The MODIS instrument includes a total of 36 spectral channels ranging from visible to thermal-infrared
spectrum, providing retrievals of atmospheric properties including aerosol optical depth over land and oceans (Remer et al.,
100 2005; 2013). The Collection 6.1 Aqua MODIS Dark Target (DT) data (DOI: 10.5067/MODIS/MYD04_L2.061), which
were used in this study, include AOD retrievals at 7 different wavelengths (0.47, 0.55, 0.66, 0.86, 1.24, 1.63, 2.11 μm) over
global oceans and 3 wavelengths over land (0.47, 0.55, 0.66 μm), with a spatial resolution at nadir of 10 km (Levy et al.,



2013). Since the reflectance-based VIIRS DNB AOD retrievals developed in this study are available at the 0.55 μm wavelength, Effective Optical Depth Average Ocean data from MODIS were used for intercomparison with nighttime
105 reflectance-based VIIRS AOD retrievals. The MODIS data used in this study were obtained from the NASA Level-1 and Atmosphere Archive & Distribution System Distributed Active Archive Center (<https://ladsweb.modaps.eosdis.nasa.gov/>; last access: Apr 16, 2026).

2.3 AERONET Data

The cloud screened, quality assured Version 3, Level 2.0 nighttime AERONET data and Version 3, Level 2.0
110 daytime AERONET data from the Dakar, Senegal station (14.4° N , 17.0° W) were used to evaluate the VIIRS retrieved AOD data. Through directly measuring attenuated moonlight or daytime sky radiance, AERONET AOD data are available at several wavelengths from 340 nm to 1020 nm (Holben et al., 1998; Giles et al., 2019). AOD retrievals at 0.675 μm and 0.5 μm from both the daytime and nighttime AERONET AOD products were used to assess the performance of the VIIRS retrieved AODs from the two different retrieval methods. The AERONET datasets used in this study were obtained from the
115 AERONET website (aeronet.gsfc.nasa.gov; last access: Apr 16, 2026). In addition, both daytime and nighttime averages of AERONET AOD data were also downloaded from the AERONET website to investigate the difference in day and night AERONET data over the study region.

2.4 Models

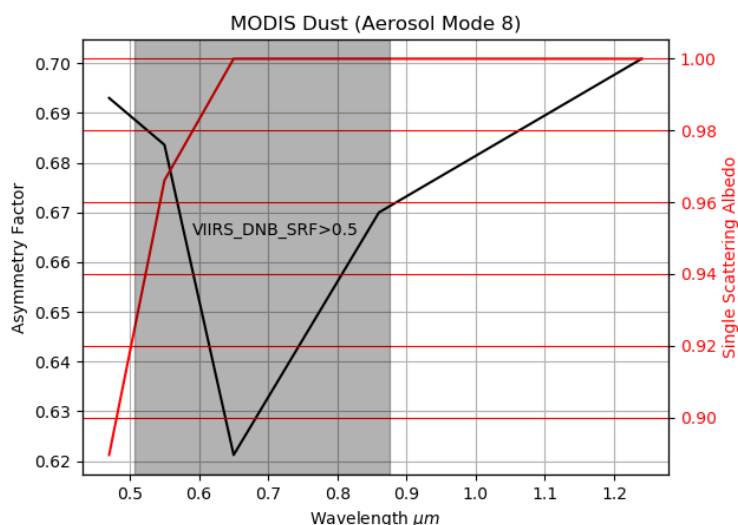
VIIRS DNB data include calibrated TOA upwelling radiances, that is a strong function of moon phase and linked to
120 parameters such as moon fraction and lunar zenith angle. To port daytime AOD retrieval methods for nighttime events, an estimation of TOA downwelling moon flux for a given observing condition is needed. For this study, we used the Miller and Tuner model (Miller and Turner, 2009), that estimates TOA downwelling fluxes based on spectral moon albedo, earth-moon-sun geometries, moon phase and the earth and sun distance. By applying the VIIRS DNB sensor response function, VIIRS DNB reflectance can be derived using the Miller and Tuner model, and by using measured VIIRS DNB radiances as
125 inputs (Miller and Turner, 2009).

To perform AOD retrievals, the Santa Barbara Distort Radiative Transfer (SBDART) model (Ricchiazzi et al., 1998) was used to simulate VIIRS DNB received TOA reflectances over ocean scenes. The inputs for the radiative transfer



130 model include surface properties, viewing geometries and atmospheric and aerosol conditions. Here we used ocean properties included in the SBDART model. The viewing geometries are from satellite ephemeris data. A standard atmospheric profile (Ricchiazzi et al., 1998) is assumed in which the mean vertical distribution of atmospheric properties (e.g., temperature) represents that of annual mid-latitude conditions. For consistency in dust aerosol optical properties, we applied MODIS Collection 6 (C6) Dark-Target (DT) over-ocean algorithm values of aerosol physical properties including refractive index, effective radius, and radii standard deviation values were obtained from wavelength ranges from 0.47 μm – 2.11 μm (e.g., Figure 1). Using this information, for coarse mode aerosols, T-Matrix (Mischenko et al., 1996) calculations were performed by the research team to estimate dust optical properties including phase function, single scattering albedo, extinction cross section, and scattering cross section, assuming dust aerosols are spherical. Lastly, SBDART is designed for daytime simulations. To perform nighttime simulations, the spectral TOA downwelling solar spectral irradiances were replaced by the spectral TOA downwelling lunar spectral irradiances with detailed discussed in Section 3.1.

140



145

Figure 1. Dust aerosol properties as a function of wavelength used in this study. This dust aerosol optical property data is obtained from the aerosol optical model 8 used in constructing the MODIS Dark Target products

150 3 Methodology

The VIIRS DNB nighttime observations, MODIS daytime observations, AERONET nighttime Lunar Provisional and daytime quality assured AERONET data were acquired for the 2017 and 2018 calendar years over the Dakar, Senegal region. Both the city light retrieval method and the lunar reflectance-based retrieval method were applied to VIIRS DNB



data for aerosol retrievals as described below. Co-located MODIS and AERONET data were used for evaluating/validating
155 VIIRS retrieved AOD values from this study.

3.1 Lunar Reflectance-Based Retrieval Method

3.1.1 Retrieval Approach

As it is challenging to perform passive-based aerosol retrievals over bright surfaces such as desert regions using the
reflectance-based method, only over-ocean, nighttime, assumed-dust, aerosol retrievals were applied using the lunar
160 reflectance-based method. Here we used the ocean surface reflectance model included in the SBDART model (Ricchiazzi et
al., 1998) and changes in ocean optical properties (e.g. suspended sediments) are not considered. Additionally, while water
vapor impacts the growth of hygroscopic aerosols, the influence of water vapor on AOD retrievals is considered marginal at
the visible spectrum (Knapp et al., 2002). The lunar reflectance-based method is almost identical to the reflectance method
implemented for daytime aerosol retrievals (e.g. MODIS) but for a single channel. Different from the daytime solar-based
165 reflectance method, reflected moonlight, instead of reflected sunlight, is used for estimating TOA reflectance for the
nighttime AOD retrieval process. To perform the retrieval, the VIIRS DNB measured reflectance values are inter-compared
with precomputed reflectance values from a look-up-table (LUT) for different atmospheric and aerosol conditions. The LUT
values were computed using SBDART model (Ricchiazzi et al., 1998) with details listed in Section 2. The LUT includes
precomputed reflectance based on aerosol properties, varying viewing geometries (lunar zenith angle, sensor zenith angle,
170 relative azimuth angle), as well as surface conditions using SBDART runs. In this study, to construct the LUTs, SBDART
simulations were performed for over-ocean dust cases for 18 AOD, 9 lunar zenith angle, 7 sensor zenith angle and 12
relative zenith angle ranges.

As SBDART is designed with solar spectral irradiance models for radiative transfer in the visible spectrum, to
create an AOD look-up-table for nighttime retrievals, a lunar spectral irradiance model is needed. This was created by
175 normalizing the 5s solar model included within SBDART using the mean sun-moon-earth distance and the lunar albedo from
Miller and Turner (2009). To simulate VIIRS DNB radiance, the VIIRS DNB sensor spectral response function was also
used to determine upwelling and downwelling TOA radiance. TOA reflectance is derived by dividing the upwelling radiance
multiplied by π by the downwelling lunar flux. Note that this approach does not directly account for the variations in sun-



180 moon-earth distance and lunar phase. Yet, both affect TOA downwelling flux, and should be accounted for indirectly by using TOA reflectance ($\pi \times \text{TOA upwelling radiance} / \text{TOA downwelling flux}$) as both the TOA upwelling radiance (part of the numerator) and the TOA downwelling flux (the denominator term) terms shall be scaled by the above-mentioned variations.

3.1.2 Quality Check for the Lunar Reflectance-Based Retrieval Method

Several quality check processes were implemented for removing less-ideal retrieving conditions, including lunar fractional illumination, glint angle, and data count checks. The lunar fractional illumination was used as a determination for the fullness of the moon on a range of 0 (new moon) – 1 (full moon). Since lunar phase is constant regardless of location on Earth, a base location of the Prime Meridian ($0^\circ, 0^\circ$) was used as the location for the lunar fractional illumination retrieval. Still, nights with less sufficient moonlight need to be excluded for reliable nighttime aerosol retrievals. For example, for lunar fractional illumination changes from 1 to 0.5, the VIIRS DNB received radiance values can be decreased by ~90% (Cao et al., 2019), which significantly reduces the signal-to-noise ratio for reliable aerosol retrievals. Thus, for this study, only VIIRS DNB data with lunar fractional illumination values larger than 0.50 are used for AOD retrievals. For fractional illuminations below 0.5, sensor noise is comparable to the incoming reflected lunar irradiance resulting in “noisy” pixels with large reflectance values (see discussions related to Figure 7). Note that for lunar fractional illumination ranges from 0.85 to 1.0 (e.g. Figure 6), which is preferred for nighttime aerosol retrievals, sufficient TOA incoming moonlight accounts for 7-9 days per month (or 84-108 days per year).

Similar to daytime aerosol retrievals, where regions with sun glint are excluded due to strong glint reflectance, regions with moon glint are also excluded for nighttime aerosol retrievals. Also, similar to daytime aerosol retrievals (Jackson et al., 2013), VIIRS DNB data with lunar glint angles less than 40° are excluded by this study. Moon glint regions are associated with higher-than-normal TOA upwelling radiance/reflectance as observed from VIIRS, which can introduce high biases in VIIRS DNB based nighttime aerosol retrievals and thus need to be removed in the retrieval process.



3.1.3 Cloud Screening for the Lunar Reflectance-Based Retrieval Method

Cloud contamination is a persistent problem in daytime aerosol retrievals (e.g., Reid et al., 2022) and is even more problematic for nighttime aerosol retrievals using VIIRS DNB data. This is because unlike daytime retrievals that can utilize the high-resolution, visible and near IR channel-based cloud mask, only VIIRS DNB and VIIRS mid/thermal IR channels
205 can be used to detect clouds at nighttime. Nighttime cloud observations are challenged to detect small, low and thin clouds, especially at lower lunar fractional illumination values. Further, thick aerosol plumes may have similar reflectivity as clouds and can be misclassified as “cloud” for VIIRS nighttime cloud products. Thus, various cloud screening steps were applied. Naturally, cloud fraction as reported from the nighttime VIIRS cloud products (e.g., Kopp et al., 2014) was used to screen potential cloud contaminated data points. To further excluding cloud contaminated data, a spatial coherence test for the
210 VIIRS DNB data was also implemented.

The concept behind the spatial coherence test assumes that cloud contaminated regions have larger spatial variance than clear and aerosol polluted regions. Note that a similar concept was also applied for cloud-clearing daytime MODIS aerosol retrievals (Martins et al., 2002). In this method, retrievals were conducted at a 10 x 10-pixel domain. Both the standard deviation of a 10×10-pixel area and the averaged cloud fraction of the 10 x 10-pixel domain (based on the VIIRS
215 cloud products) were computed. A set of cloud fraction thresholds (0.2-0.8) and a set of standard deviation thresholds (0.01-0.02) were used for cloud screening and the sensitivity of the thresholds chosen are mentioned in Section 3. Also, if the count of pixels within a 10 x 10 aggregated granule is than 25 (e.g., missing pixels) no retrieval is conducted.

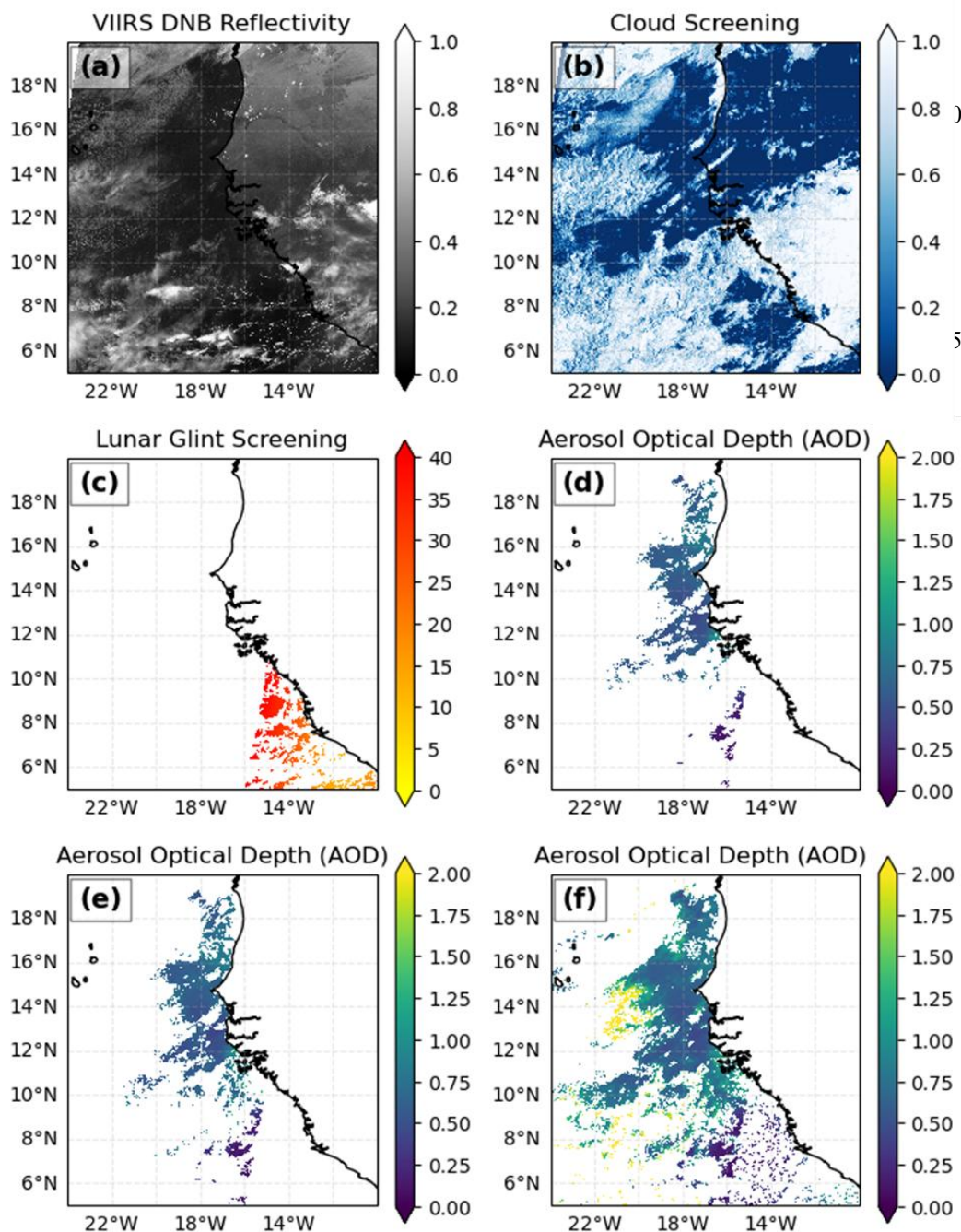


Figure 2. a) Lunar reflectance from 27 Oct 2018, b) cloud mask for the same data as a) using a standard deviation threshold of 0.01 and cloud fraction threshold of 0.6, c) glint mask, d) AOD ($0.55 \mu\text{m}$) retrievals for the same image as a), with the use of the standard deviation threshold of 0.01 and cloud fraction threshold of 0.2 for cloud masking, e) similar to d) but with the use of a standard deviation threshold of 0.01 and cloud fraction threshold of 0.6 for cloud masking, f) similar to d) but with the use of a standard deviation threshold of 0.02 and cloud fraction threshold of 0.8 for cloud masking



250

Figure 2 shows an example of nighttime AOD retrievals for a case from 27 October 2018 illustrating the use of varying cloud screening thresholds. While cloud contamination is clearly visible using a cloud fraction threshold of 0.8 and a standard deviation threshold of 0.2 (Figure 2f), the use of a very stringent cloud fraction threshold of 0.2 and a standard deviation threshold of 0.01 exclude some valid AOD retrievals (Figure 2d). To maintain sufficient retrievals while suppressing cloud contamination, an optimal section of thresholds for cloud screening is needed, which is discussed in detail in Section 4.

255

3.2 City Light-Based Retrieval Method

260 Equation 1:

$$I_{sat} = I_s e^{-\tau/\mu} + I_s T(\mu) + I_p \quad (1)$$

where I_{sat} is the radiance received by the VIIRS instrument. $I_s e^{-\tau/\mu}$ is the direct upwelling surface light emission where μ is the cosine of the viewing angle. τ is the total column optical depth and I_s is the surface upward irradiance for cloud-free sky. $I_s T(\mu)$ is the upwelling surface light emission through diffuse transmittance with $T(\mu)$ being the diffuse transmittance, and I_p is the path irradiance source. Equation 1 shows that the observed radiance includes both direct and diffused radiation from the atmosphere, Earth's surface, and artificial light sources.

265

The optical depth of an atmosphere column can thus be derived, based on Eq. 2 (derived from Eq. 1; Johnson et al., 2013; McHardy et al., 2015; Zhang et al., 2019; 2025)

$$\tau = \mu \ln \frac{\Delta I_a}{k \Delta I_{sat} (1 - \bar{r}_s)} \quad (2)$$

270

where τ is the nighttime column integrated aerosol optical depth, k is a correction factor for the diffuse transmittance, derived from the 6S radiative transfer model for a standard atmosphere (Vermote et al., 1997; Johnson et al., 2013), ΔI_{sat} is the variance in TOA radiance for an artificial light source for cloud-free conditions over an artificial light source, ΔI_a is the variance in TOA radiance for an artificial light source for aerosol and cloud-free conditions, and the \bar{r}_s term is the reflected



275 surface upward radiance by the aerosol layer and is treated as negligible in this study. τ is a summation of optical depth from aerosols, as well as Rayleigh scattering and absorption optical depth for gas species (Zhang et al., 2019).

Similar to the previous method, quality check and cloud screening steps were applied. First, missing or out-of-range data pixels were removed, along with pixels that have poor calibration quality or exhibited saturation. This process is adopted from Zhang et al., (2019) and requires a threshold-based screening of the solar zenith angle for a given pixel. For 280 each pixel, a solar zenith angle greater than 102° must be observed to eliminate solar and twilight contamination. Following cloud screening and the previous quality assurance steps, artificial light source pixels were identified through a threshold-based method (Johnson et al., 2013; Zhang et al., 2019). For a pixel to be determined as an artificial light source pixel, the radiance of a pixel must be greater than 1.5 times the mean granule cloud-free background radiances. Various cloud screening methods, following Zhang et al., (2019) were also implemented.

285 The artificial light based AOD retrieval method was applied to data over Dakar, Senegal for the years of 2017 and 2018. Retrieved VIIRS AOD ($0.7 \mu\text{m}$) from the city light method were intercompared with both daytime and nighttime AERONET retrievals and the AOD retrievals from the previously mentioned lunar reflectance based nighttime aerosol retrieval method ($0.675 \mu\text{m}$).

3.3 AERONET AOD Co-location Technique

290 As described earlier, the AERONET AOD data used in this study are nighttime Level 2.0 Lunar data and daytime Level 2.0 data taken from the 675 nm ($0.675 \mu\text{m}$) and 500 nm ($0.5 \mu\text{m}$) wavelengths retrieved at the Dakar, Senegal (14.4° N , 17.0° W) station for the calendar years of 2017 and 2018. The city light-based AOD retrievals are available at $0.7 \mu\text{m}$, so AERONET AOD data at $0.675 \mu\text{m}$ were used for inter-comparison purposes. The lunar reflectance-based AOD retrievals are available at $0.55 \mu\text{m}$ thus, to inter-compare VIIRS and AERONET AODs, the AERONET data from both $0.5 \mu\text{m}$ and 0.675 295 μm were used and interpolated to estimate AERONET AOD retrievals at $0.55 \mu\text{m}$ following a method as described in Shi et al., (2011).

The AERONET co-location technique used in this study is based upon the co-location techniques introduced in previous studies (Zhang et al., 2019). To be specific, only VIIRS and lunar AERONET data pairs that have a temporal difference within ± 30 minutes (0.02 Julian Days) and a spatial difference within 1° (Latitude/Longitude; Euclidean



300 distance) were used. To compare with daytime AERONET data, the temporal and spatial windows are set to +/- 24 hours for a given nighttime VIIRS AOD retrieval and 1° (Latitude/Longitude; Euclidean distance) respectively. Additionally, for daytime AERONET AOD comparisons with city light-based and lunar reflectance-based retrieved AOD, the AERONET AOD retrieved from the same day and the previous day (+/- 24 hours) are compared and if the difference in daytime AERONET AODs is within 0.2, a comparison with the city light-based or lunar reflectance-based AOD is attempted.

305 **3.4 MODIS AOD Co-location Technique**

The aforementioned MODIS AOD data were also used to evaluate the performance of the lunar reflectance-based VIIRS AOD retrievals. Although only daytime AOD retrievals are available from MODIS, different from AERONET data which are only available at sporadic locations, MODIS data can be used for cross-evaluating VIIRS AOD retrievals over a large spatial domain. For this effort, MODIS DT AOD data were used to inter-compare with the reflectance-based VIIRS
310 DNB AOD retrievals, which are available at 0.55 μm . To co-locate the MODIS and VIIRS data spatially, both MODIS and VIIRS AOD data were further averaged into 0.5° x 0.5° (Latitude/Longitude) aggregates. Only aggregates at the same 0.5° x 0.5° (Latitude/Longitude) bins were further used. To co-locate the MODIS and VIIRS data temporally, the MODIS AOD retrievals from the same day as the VIIRS AOD retrievals were averaged to represent the AOD for the given bin. We also compared daytime average AERONET AOD data with the same days average MODIS AOD data that were within 0.5°
315 (Latitude/Longitude) Euclidean distance from the Dakar, Senegal AERONET station over the study period.

3.5 Comparison of Lunar Reflectance-Based and City Light-Based Retrieval Methods

One of the goals in this study is to intercompare the lunar reflectance-based and the retrieved city light-based AOD over the Dakar, Senegal region. For the city light-based method, retrievals were performed at a spatial resolution of 25×25 km². Given the center point of 14.7231° N, -17.4604° S, artificial lights from Dakar, Senegal spanned across a total of five
320 25×25 km² domains. Retrievals from the 25×25 km² domains were averaged to represent the city light-based AOD retrieval for a given night. For the reflectance-based method, all available retrievals within a 1° x 1° (latitude/longitude) bounding box over Dakar, Senegal (14.7231° N, -17.4604° S) were averaged to represent the lunar reflectance-based AOD retrieval for the night. AOD retrievals from the two different methods were further inter-compared over Dakar to determine the frequency and performance of the moonlight and city light-based retrieval methods. For this, time series analysis was also conducted



325 using AERONET and VIIRS DNB AOD data at $0.675 \mu\text{m}$ over Dakar, Senegal for 2017 and 2018. Since, the VIIRS DNB
lunar reflectance-based retrieved AODs are completed at $0.55 \mu\text{m}$, a ratio, which is the averaged difference between the
Lunar AERONET AODs at $0.55 \mu\text{m}$ and $0.675 \mu\text{m}$, was precomputed. This ratio is used to scale the VIIRS DNB lunar
reflectance retrieved AODs from $0.55 \mu\text{m}$ to $0.675 \mu\text{m}$ for inter-comparison with the other AOD data used in this study.

4 Results

330 In this section, nighttime aerosol retrievals from both the lunar reflectance method and city light methods were
attempted using VIIRS DNB data near the Dakar, Senegal region for 2017 and 2018. Inter-comparisons with
nighttime/daytime AERONET and daytime MODIS AOD retrievals were performed. Issues and limitations for each method
were also explored.

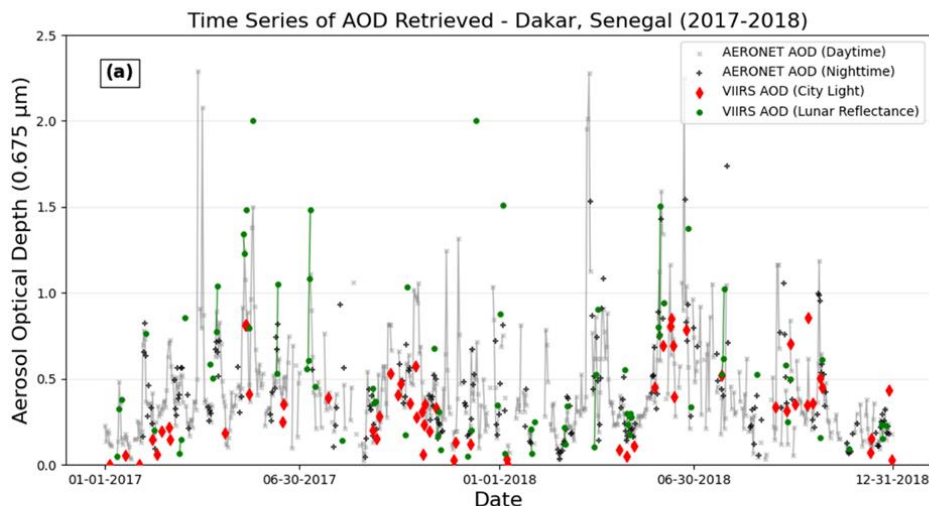
4.1 Comparison of Nighttime City Light and Lunar Reflectance-Based AOD Retrievals

335 As the first step, we intercompare AOD retrievals from the reflectance based and the city light based AOD
retrievals with a time series of solar and lunar AERONET measurements as shown in Figure 3a. AOD retrievals from the
lunar reflectance-based method were conducted using a standard deviation threshold of 0.01 and cloud fraction threshold of
0.2. Detailed comparisons between AOD retrievals from both methods and AERONET and MODIS AOD data under
difference observing conditions can also be found in later sections (e.g., Sections 4.2, 4.3 and 4.4). As suggested from
340 Figure 3a, while AOD retrievals from both methods compare reasonably with AERONET AODs, underestimations and
overestimates are observable, including some significant outliers. In addition, there are only few nights that AOD retrievals
from both methods are available, raising a sampling issue for both methods.

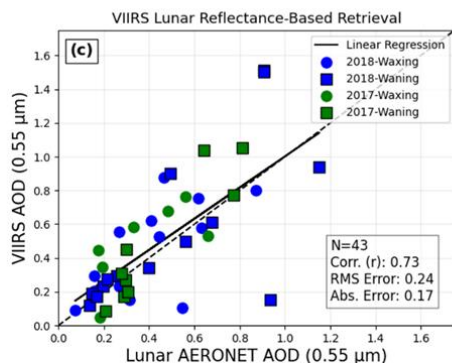
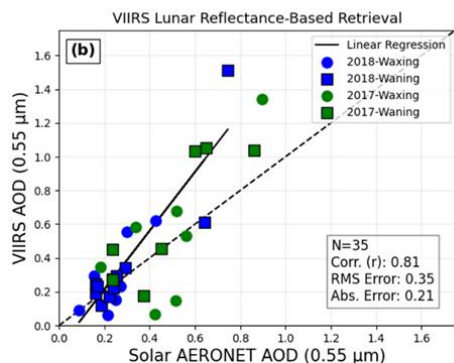


345

350



355



360

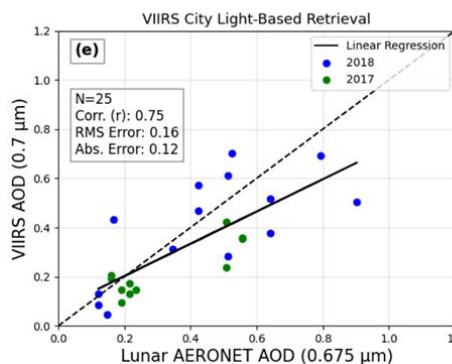
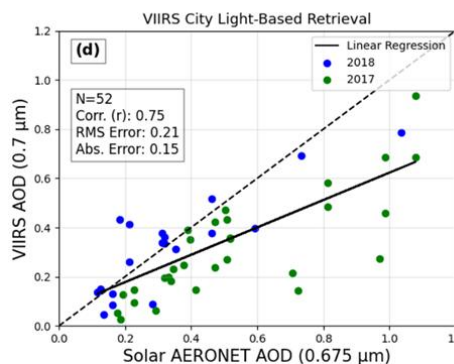


Figure 3. a) Time series of days/nights with AERONET daytime AOD ($0.675 \mu\text{m}$), AERONET nighttime AOD ($0.675 \mu\text{m}$), VIIRS lunar reflectance-based retrieved AOD ($0.675 \mu\text{m}$) and VIIRS city light-based retrieved AOD ($0.7 \mu\text{m}$) from Dakar, Senegal for 2017 and 2018. Co-located comparisons of b) daytime AERONET AOD and c) nighttime AERONET AOD and VIIRS DNB lunar reflectance-based AOD ($0.55 \mu\text{m}$) retrievals with a standard deviation threshold of 0.01 and cloud fraction threshold of 0.2. Also included are co-located comparisons of city light retrieved AOD with d) daytime and e) nighttime AERONET AOD from Dakar, Senegal for 2017 and 2018.



For example, for 2018, 279 days are observed by daytime AERONET AOD, 117 nights are observed by nighttime
365 AERONET AOD, yet only 25 nights have completed retrievals of AOD via the city light-based retrieval method, and 37
nights have completed retrievals of AOD via the lunar reflectance-based retrieval method. For 2017, 38 nights have
completed retrievals using the lunar reflectance-based method, 33 nights have completed AOD retrievals via the city light-
based retrieval method, 86 nights are observed by nighttime AERONET AOD, and 292 are observed by daytime AERONET
AOD. It is not surprising that the nighttime lunar provisional AERONET AOD and the lunar reflectance-based AOD
370 retrieval method have some of the fewest numbers of retrievals since both require moonlight to provide adequate lighting
conditions for the retrieval of AOD. Furthermore, the lunar reflectance-based AOD retrieval method features several quality
assurance steps that implement the VIIRS cloud product and contain screenings for lunar glint regions that further exclude
additional nights from the study. The AERONET and city light retrieved AODs do contain cloud screening steps but not the
moon-glint screening step as these retrievals took place on land surfaces. Furthermore, ideal lunar reflectance-based AOD
375 retrievals require nights with the lunar fractional illumination to be over 85%, which limits retrievals to 7-9 nights per month
or 84-108 nights per year. The city light-based method, on the other hand, could be implemented regardless of moon status.

Regardless of limitations as mentioned above, both the reflected moonlight as well as the city light-based methods
have some merit in retrieving nighttime AOD by using observations from the VIIRS DNB. Future studies are needed to
further explore the pros and cons of both methods and for developing a suitable method for future operational based
380 applications. There are only eight nights with retrievals from both methods, with three nights in 2017 and five nights
occurring in 2018 with a correlation of 0.59 and a mean difference of 0.14 in terms of AOD. 68 and 57 nights occur with
retrievals from any one of the retrievals for 2017 and 2018 respectively, indicating that the combined use of the two methods
may double the data sampling rates for nighttime AODs using VIIRS DNB data.

4.2 VIIRS DNB AOD Lunar Reflectance-Based AOD Retrieval Comparisons with Co-located AERONET AOD 385 Retrievals

VIIRS DNB AOD retrievals from the lunar reflectance-based nighttime AOD (0.55 μm) retrieval method from
varying cloud screening thresholds were inter-compared with Level 2.0 daytime AERONET AOD and Level 2.0 Lunar
AERONET AOD data from Dakar, Senegal as shown in Table 1. An example of these comparisons is shown in Figure 3b-c



using VIIRS AOD retrievals with a standard deviation threshold of 0.01 and cloud fraction threshold of 0.2. Figure 3b
390 implies that the assumption that nighttime is similar to daytime is prone to error, as larger RMS (0.35) and absolute (0.21)
errors are found between nighttime VIIRS AOD and daytime AERONET AOD (Figure 3b). The scatter plot of VIIRS DNB
and lunar AERONET AOD for 2017-2018 is shown in Figure 3c, for which a slope of 0.95, an RMS error of 0.24 and an
absolute error of 0.17 are found, indicating the feasibility of using lunar reflectance for aerosol retrievals.

The comparison study was conducted as a function of cloud screening thresholds as mentioned in Section 2 to
395 evaluate the impact of and to select the best combination of cloud screening thresholds for AOD retrievals as shown in Table
1. Table 1 shows the comparison of nighttime AERONET AOD ($0.55 \mu\text{m}$) and VIIRS DNB lunar reflectance-based
retrieved AOD ($0.55 \mu\text{m}$) as functions of the standard deviation threshold of 0.01-0.02 and the cloud fraction threshold of
0.2-0.8 for using data from 2017 and 2018. The number of valid collocated pairs decreased from 69 to 68 for cloud fraction
threshold of 0.8 to 0.2 for a fixed standard deviation threshold of 0.02 with a decrease in absolute error from 0.23 to 0.22.
400 The use of a more stringent standard deviation threshold of 0.01 lowered RMSE and absolute errors to 0.25 and 0.17,
respectively, yet reducing data pairs to 43. Clearly, better performance is expected with more stringent cloud screening at the
cost of data loss. The optimal threshold is found to be a standard deviation threshold of 0.01 and cloud fraction threshold of
0.2.

In addition, the Miller and Turner (2009) model was used to estimate TOA downwelling lunar flux for this study.
405 In Miller and Turner (2009) model, different correcting factors were applied to the waxing and waning conditions. Thus, the
comparison of VIIRS and AERONET AOD data was also conducted for both the waxing (filled circles) and waning (filled
squares) conditions as shown in Figure 3 (e.g., Figs. 3b and 3c). As shown in Figure 3, no apparent differences are found for
nighttime AOD retrievals using the lunar reflectance-based method for both waxing and waning phases. In addition to lunar
conditions, we also wanted to determine the frequency of AOD retrievals completed above/below a fractional illumination of
410 0.85. One collocated nighttime AOD retrieval was completed from 2017-2018 under a lunar fractional illumination of 0.85,
with an AERONET lunar AOD of 0.20, VIIRS DNB AOD of 0.11, and lunar fractional illumination of 0.73. Forty-two other
collocated retrievals using a standard deviation of 0.01 and cloud fraction threshold of 0.2 were completed with lunar



fractional illumination values greater than 0.85. VIIRS DNB AOD retrievals completed with a lunar illumination greater than 0.85 for 2017-2018 have a RMS error of 0.25 and absolute error of 0.17.

Standard Deviation Threshold	Cloud Fraction Threshold	Data Count	Root-Mean-Square Error	Absolute Error	Correlation (r)	r ² Value
Solar AERONET AOD						
0.01	0.2	35	0.35	0.21	0.81	0.65
	0.4	38	0.39	0.24	0.81	0.65
	0.6	38	0.58	0.35	0.63	0.39
	0.8	44	0.61	0.38	0.67	0.44
0.02	0.2	57	0.45	0.30	0.69	0.47
	0.4	58	0.47	0.32	0.70	0.49
	0.6	60	0.57	0.37	0.59	0.34
	0.8	66	0.68	0.46	0.58	0.33
Lunar AERONET AOD						
0.01	0.2	43	0.24	0.17	0.73	0.53
	0.4	43	0.25	0.17	0.72	0.51
	0.6	45	0.25	0.18	0.72	0.51
	0.8	46	0.25	0.18	0.77	0.59
0.02	0.2	68	0.30	0.22	0.72	0.51
	0.4	68	0.30	0.22	0.73	0.53
	0.6	69	0.31	0.23	0.69	0.47
	0.8	69	0.30	0.23	0.71	0.50
MODIS AOD						
0.01	0.2	30,088	0.27	0.18	0.62	0.38
	0.4	30,685	0.28	0.19	0.61	0.37
	0.6	31,523	0.28	0.19	0.60	0.36
	0.8	32,084	0.29	0.19	0.60	0.36
0.02	0.2	49,626	0.33	0.23	0.56	0.31
	0.4	51,859	0.34	0.24	0.55	0.30
	0.6	51,595	0.34	0.24	0.55	0.30
	0.8	55,191	0.38	0.27	0.54	0.29

415

Table 1. Co-located statistical comparisons of daytime (solar) AERONET AOD (0.55 μm), nighttime (lunar) AERONET AOD (0.55 μm), MODIS AOD (0.55 μm) and VIIRS DNB lunar reflectance-based AOD (0.55 μm) retrievals from 2017 and 2018

4.3 Verification of Nighttime City Light AOD Retrievals

420

The city light-based method from this study follows the method as described in Zhang et al., (2025). As suggested in Zhang et al., (2025), the whole study area is divided into equal area grids of 25×25 km². Artificial light sources within a given 25×25 km² grid are used in the retrieval process. Note that the Dakar region is divided into five different 25×25 km² grids with grid centers at 14.462° N, 17.032° W, 14.667° N, 17.114° W, 14.702° N, 17.387° W, 14.749° N, 17.159° W, and



14.759° N, 1.353° W. Two out of five 25×25 km² grids have more than 40 detected artificial light sources. Thus, those two
425 25×25 km² grids were further used in the analysis in this study.

As previously mentioned, to verify the AOD retrieved using the city light-based method, AERONET retrieved AODs
from the Dakar, Senegal station were co-located and compared. In total, 58 nights of VIIRS DNB city light retrieved AODs
are compared against the same day's daytime AERONET AOD and nighttime AERONET retrieved AOD during 2017 and
2018. Figures 3d and 3e illustrate the comparison of AODs retrieved using the city light AOD retrieval method at 0.7 μm
430 with daytime and nighttime retrieved AODs at 0.675 μm from the AERONET station located in Dakar, Senegal for 2017 and
2018.

Figure 3d and 3e shows the comparison of the city light retrieved AODs and the attributing co-located AERONET
AODs for both nighttime and daytime observations for 2017 and 2018, respectively. Figure 3d and 3e show that the VIIRS
DNB city light-based AOD retrievals agreed reasonably well with AERONET AOD values from the Dakar, Senegal station.
435 The RMS error is on the order of 0.21, absolute error is on the order of 0.15, and the correlation is on the order of 0.75 for
daytime comparisons. For the nighttime comparison the RMS error is 0.16, absolute error is 0.12, and correlation is 0.75.
Both of which are smaller than VIIRS DNB AOD retrievals from the lunar reflectance-based method. For example, as
discussed in the previous section, the RMS and absolute errors are 0.24 and 0.17 (based on the co-located nighttime AOD
data), respectively for AOD retrievals (0.55 μm) using the reflected moonlight-based method with a standard deviation
440 threshold of 0.01 and a cloud fraction threshold of 0.2. Thus, it seems, through comparisons with nighttime AERONET data,
the city light retrieved AODs performed better than the lunar reflectance-based retrieved AODs.

It is also evident that a low bias exists for the AOD retrievals using the city light method, which is consistent with
the findings of the previous Zhang et al., (2019) study. This low bias could be attributed to several factors. First, thick
aerosol plumes are present over the Dakar, Senegal region for much of the year. Furthermore, the derived cloud- and aerosol-
445 free standard deviation of artificial light sources may not always be representative of an aerosol-free case (Zhang et al.,
2019). Additionally, high aerosol loading cases are often misrepresented by the VIIRS cloud product and are thus screened
out of the retrieval process. Data loss is experienced in this study as several quality assurance techniques are implemented
(e.g., Zhang et al., 2019).



450 Additionally, as mentioned earlier, the comparisons to daytime and nighttime AERONET AODs could not be considered ‘ground truth’ as AERONET has its own issues of representing aerosol optical depth. However, the AODs retrieved from the city light retrieval method do show skill for retrieving aerosol optical depth over artificial light sources.

4.4 VIIRS DNB AOD Lunar Reflectance-Based AOD Retrieval Comparisons with Co-located MODIS AOD Retrievals

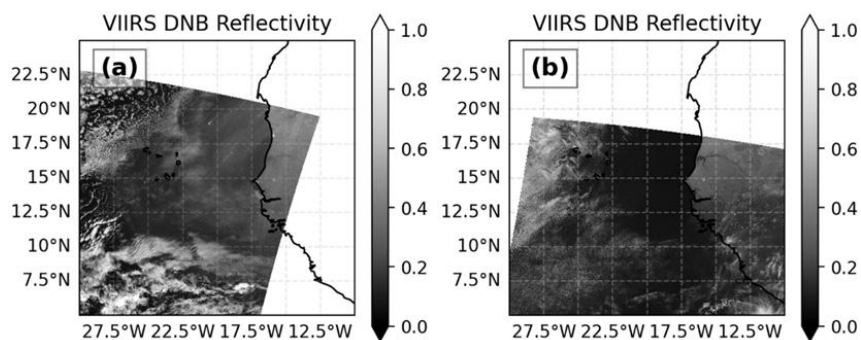
Besides using daytime and nighttime AERONET AOD data, the performance of nighttime VIIRS AOD retrievals 455 from the lunar reflectance-based method were also cross evaluated with daytime MODIS AOD retrievals. Note that there are non-trivial differences between day and nighttime AODs due to the differences in emission, transport, as well as atmospheric conditions. Still, it is to be expected some correlations exist between nighttime AOD values and daytime AOD values for the adjacent day. The comparison between MODIS (day; $0.55 \mu\text{m}$) and VIIRS (night; $0.55 \mu\text{m}$) AOD values is also used to study the data sampling rates for nighttime AOD retrievals. In addition, to fulfill the task, VIIRS DNB and 460 MODIS AOD data were aggregated to $0.5^\circ \times 0.5^\circ$ (Latitude/Longitude) resolution first, and the comparisons were conducted at the $0.5^\circ \times 0.5^\circ$ (Latitude/Longitude) grid level.

As a qualitative comparison given the day and nighttime AOD differences, Figure 4 shows an example of gridded VIIRS and MODIS AOD data from 1 June 2018 and 3 May 2018 for qualitative comparison. Figure 4e-f shows the gridded MODIS AOD data and Figure 4g-h shows the gridded VIIRS AOD data. As shown in Figure 4a, a dust plume is visible 465 along the western coast of Africa leading to elevated AOD values on 1 June in comparison to the weaker dust plume shown in Figure 4b from 3 May. In both cases, differing dust plumes are found during daytime using MODIS AOD, likely due to diurnal variations in AOD.

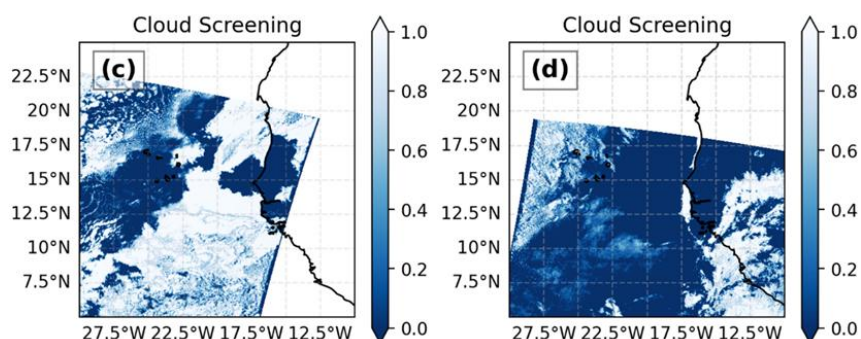
The comparisons of MODIS (daytime) and VIIRS DNB (nighttime) AOD as functions of cloud screen thresholds are also included in Table 1. Clearly, around 1000 times more pairs of MODIS and VIIRS retrievals are available in 470 comparison with the lunar AERONET and VIIRS study. Also indicated in Table 1, the more stringent the cloud threshold, the lower the RMSE and absolute errors and higher the correlation. The best cloud screen thresholds are found to be the standard deviation value of 0.01 and cloud fraction of 0.2 with a ~45% data loss comparing with the most relaxed cloud screen thresholds (standard deviation value of 0.02 and cloud fraction of 0.8).



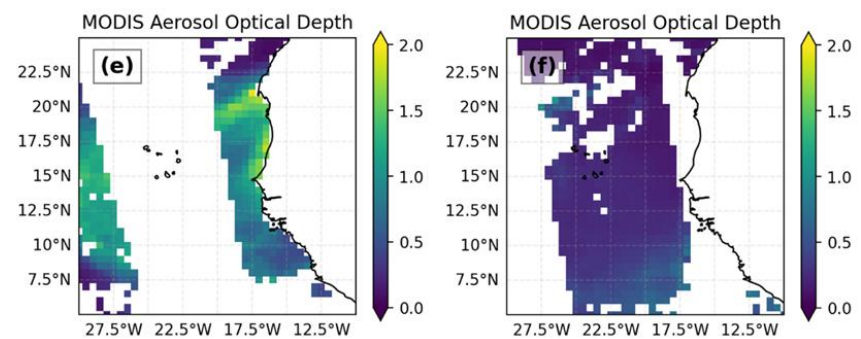
475



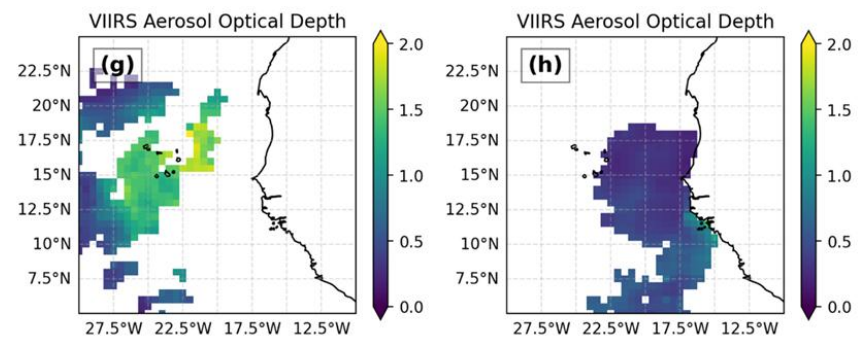
480



485



490



495

Figure 4. VIIRS DNB Reflectivity, Cloud Screening, MODIS AOD, and VIIRS DNB AOD with a standard deviation threshold of 0.01 and cloud fraction threshold of 0.2 for two dates. Panels (a), (c), (e), (g)) show 01 Jun 2018 while panels (b), (d), (f), (h)) show 03 May 2018.



500 Despite the difference in AOD values between day and night, the comparisons between daytime MODIS AOD and nighttime retrieved VIIRS DNB AOD do show some degree of agreement with a correlation range of 0.54-0.62. This suggests that the lunar reflectance-based VIIRS DNB AOD retrieval could be used to retrieve dust aerosols over an over-ocean surface, but cloud contamination, lunar phase, and lunar glint are the main uncertainty sources for lunar reflectance-based AOD retrievals. This exercise also suggests that the use of daytime-like LUTs of reflectance is applicable for nighttime AOD retrievals, as long as the retrievals are conducted using reflectance values, which are the $\pi \times$ TOA upwelling 505 radiances normalized by TOA downwelling fluxes.

4.5 Verification of AERONET AOD Retrievals and Co-located MODIS AOD Retrievals

Since both daytime AERONET and daytime MODIS DT AOD data were used to intercompare with nighttime aerosol retrievals from this study, it is necessary to investigate how representative daytime AERONET/MODIS AOD retrievals are to the given nighttime retrievals (same day) for the study region. Figure 5a shows the comparison of averaged 510 daytime and nighttime AERONET AOD measurements from the Dakar, Senegal station from 2017 and 2018. Each data point in Figure 5a represents a pair of averaged daytime AERONET AOD and nighttime AERONET AOD for the same day. A correlation of 0.84 and a RMS error of 0.14 are found between the averaged daytime and nighttime AERONET AODs for the Dakar, Senegal station for 2017 and 2018 indicating daytime AERONET AOD data has some skills in estimating nighttime AERONET AOD values.

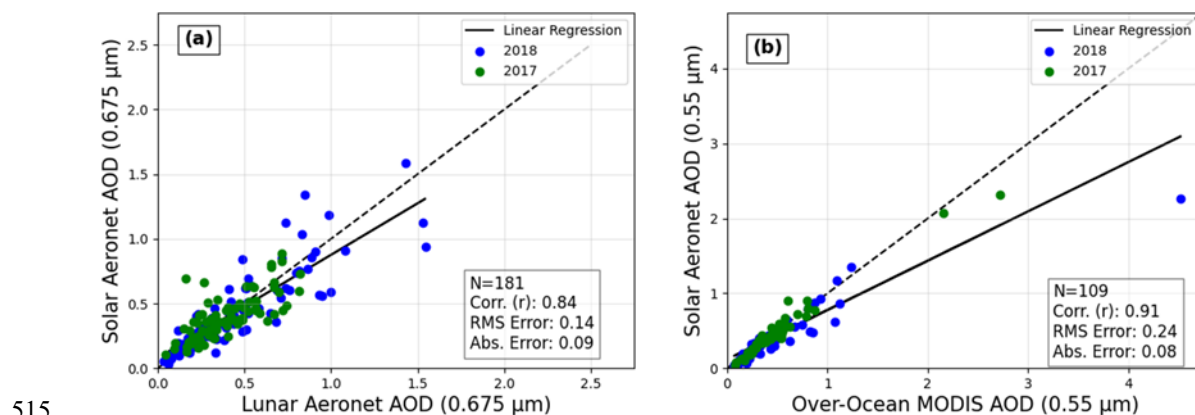


Figure 5. Co-located comparisons of a) daytime and nighttime AERONET AOD ($0.675 \mu\text{m}$) and b) daytime AERONET AOD and MODIS AOD ($0.55 \mu\text{m}$) retrievals



Figure 5b shows the co-located comparison of daytime AERONET AOD and MODIS AOD over the Dakar, Senegal
520 region for 2017 and 2018. For this comparison, MODIS AOD data within 0.5° Euclidean distance from the Dakar, Senegal
AERONET station were averaged to create a daily average to be compared with the daily averaged AERONET AOD for the
same day. This comparison shows a correlation of 0.91 and an RMS error of 0.24 indicating a considerable level of
agreement between the two datasets. A significant outlier can be observed in Figure 5b occurring on 21 June 2018 where a
significant plume of Saharan dust leads to a MODIS AOD of 4.52 and an AERONET AOD of 2.26. Figure 5 indicates that
525 both daytime AERONET and MODIS AOD retrievals can be used to assist evaluation of the retrieved nighttime VIIRS DNB
AODs.

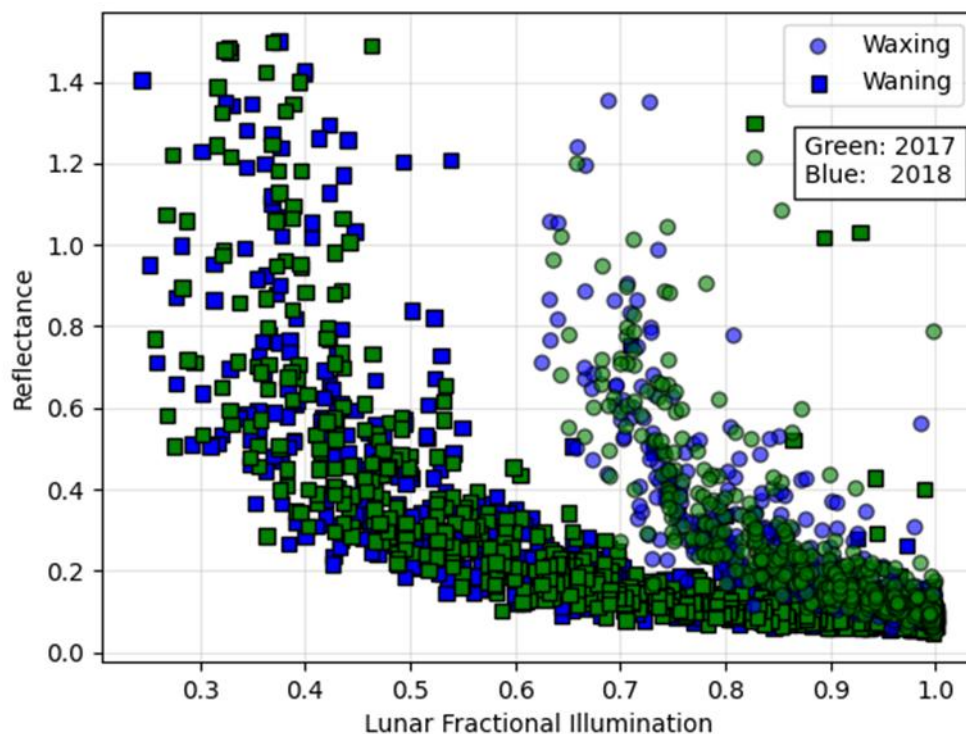
5 Discussion

5.1 Impact of Lunar Model on Data Selection and Cloud Screening

To convert from VIIRS DNB radiance to reflectance, a lunar model, which estimates TOA downward moon flux
530 under different moon status was used. Thus, the application of using the Miller-Turner lunar model for this study is explored.
For this analysis, a lunar zenith angle threshold of 80° and a satellite zenith angle of 60° was used to screen out potentially
unreliable pixels for the lunar reflectance retrieval. Figure 6 shows the cloud-cleared, over-ocean granule average reflectance
as a function of lunar fractional illumination (fraction of the moon surface illuminated, with 0 representing new moon and 1
representing full moon) for the Miller-Turner lunar reflectance model. If aerosol parameters are assumed to not be a function
535 of lunar illumination, reflectance should not see a dependence upon fractional lunar illumination. However, granule mean
reflectance increases sharply at fractional lunar illuminations below 0.85 during the waxing phase of the lunar cycle to a
physical reflectance above 1.0. Mean reflectance retrieved during the waning phase of the lunar cycle increase above 1
below a lunar fractional illumination threshold of 0.55. Dependencies on the lunar cycle, waxing or waning, can cause
differences in mean granule reflectance, primarily due to lunar zenith angle and partially due to the zenith angle of the
540 sensor. Between the two lunar phases, fewer granules are retrieved during the waxing phase of the lunar cycle than that of
the waning phase. Ultimately, random noise produced by VIIRS DNB depending on viewing and lunar geometries limit the



effectiveness of the lunar reflectance-based AOD retrieval method. Visual inspection of granule reflectance shows random noise due to decreased signal-to-noise ratios when incident lunar light is limited (e.g., Figure 7).

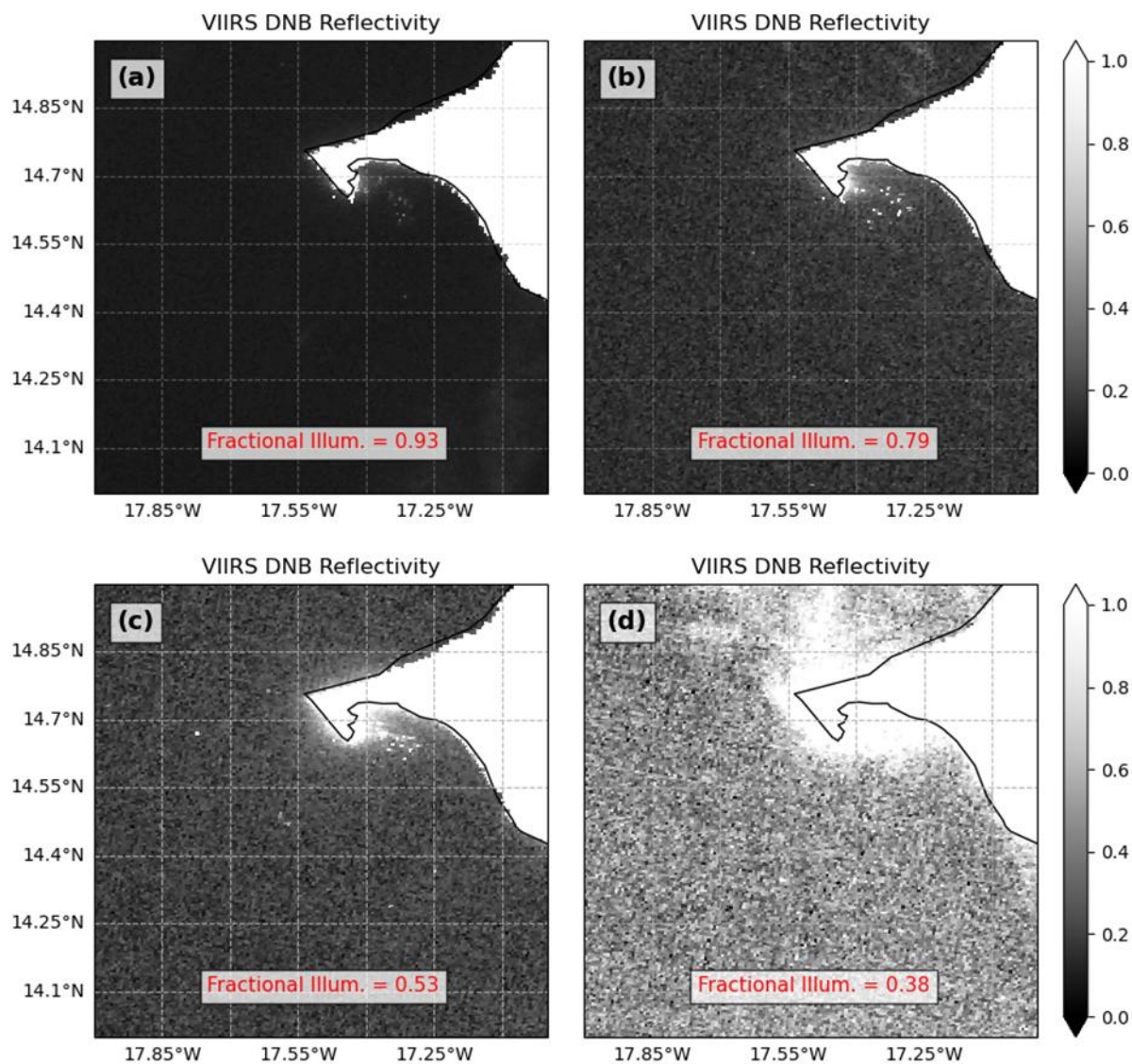


545

Figure 6. Granule mean reflectance versus lunar phase (fractional illumination) using the Miller-Turner lunar model for 2017 and 2018 over the study region

This exercise highlights limitations in the currently used lunar model. It is for this reason, for over ocean nighttime AOD retrievals using VIIRS DNB data, the optimal lunar fractional illumination range is from 0.85 to 1. It is worth noting that the city light-based method derived AOD values are based on the contrast within a given artificial light source and thus is negligibly impacted by uncertainties in lunar models and can be applied to nights with near-zero lunar phase angles. Still, Figure 7 indicates the need for careful qualification of lunar models for nighttime related applications that rely on using moonlight.

550



555 **Figure 7.** a) VIIRS DNB image for 27 Oct 2018 with a lunar fractional illumination of 0.93, b) VIIRS DNB image for 26 Feb 2018 with
a lunar fractional illumination of 0.79, c) VIIRS DNB image for 09 Mar 2018 with a lunar fractional illumination of 0.53 and d) VIIRS
560 DNB image for 01 Dec 2018 with a lunar fractional illumination of 0.38

6 Conclusion

Using two years (2017 & 2018) of VIIRS DNB data and AERONET AOD data over the Dakar, Senegal region,
560 nighttime AOD retrievals were performed using both the city light and the lunar reflectance methods. Limitations and issues



for both retrieval methods were explored. AOD retrievals from both methods were also inter-compared. This study found that:

- 1). Both the lunar reflectance-based and city light-based methods have some skills in retrieving nighttime AODs. Validated against ground-based lunar AERONET data, the correlation, RMS error and absolute errors are 0.73, 0.24 and 0.17 for 43
565 co-located AOD retrievals using the lunar reflectance-based retrieval method for 2017 and 2018 data (standard deviation threshold of 0.1 and cloud fraction threshold of 0.2; 0.55 μm). Additionally, the correlation, RMS error and absolute errors are 0.75, 0.16, and 0.11 for 25 co-located AOD retrievals using the city light-based method (0.7 μm) for 2017 and 2018.
- 2) This study confirms that if reflectance values ($\pi \times \text{TOA upwelling radiance} / \text{TOA downwelling flux}$) from the VIIRS DNB data can be obtained, LUT for reflectance-based daytime AOD retrieval using the VIIRS DNB can be applied to nighttime
570 by normalizing by the lunar albedo integrated over the VIIRS DNB spectral response. For example, retrieval methods developed for using daytime VIIRS DNB data (or a given sensor that is sensible to both day and night lights, capable of observing earth-atmospheric system using single channel, multiple, or hyperspectral channels) can be adapted for AOD retrievals using nighttime VIIRS DNB reflectance data (or reflectance data from the given sensor) with the use of the reflectance-based method.
- 3) AOD retrievals using the lunar reflectance-based methods are often limited by cloud contamination, moon glint and lunar
575 phase. Since only nights with sufficient moonlight could be used in the retrieval process, 7-9 nights per month or 84-108 nights per year are qualified under this requirement. This limits the application of the lunar reflectance-based AOD retrieval method. In comparison, the city light-based method can be applied at nights with or without moon light. Still, only a very limited number of AOD retrievals (33 in 2017, 25 in 2018) from the city light-based methods were derived. As many nights
580 were excluded due to cloud screening and QA steps.
- 4) There are still noticeable uncertainties in lunar models that can affect nighttime AOD retrievals using the reflectance-based method, especially for nights with lunar phase angle less than 0.85. Additional refinements in lunar models are needed in future studies.



585 5). This study highlights the limitation of both nighttime retrievals and demonstrates hopes for nighttime AOD retrievals using VIIRS DNB data. Perhaps combined retrievals from both methods could provide better data coverage, which deserves further exploration in a future study.



Code and data availability

590 The Aqua MODIS data used in this study were obtained from the NASA Level-1 and Atmosphere Archive & Distribution System Distributed Active Archive Center (<https://ladsweb.modaps.eosdis.nasa.gov/>). The AERONET Level 2 nighttime and daytime datasets used in this study were obtained from the AERONET website (aeronet.gsfc.nasa.gov). The VIIRS data for this study were obtained from the NOAA Comprehensive Large Array-Data Stewardship System (NOAA CLASS; <https://www.avl.class.noaa.gov/saa/products/>). The SBDART Radiative Transfer model (Ricchiazzi et al., 1998; <https://github.com/paulricchiazzi/SBDART>) and T-Matrix model (Mischenko et al., 1996) are publicly available software.

Author contributions

600 Authors J. Zhang and J. W. Marquis designed the study. Author A. Schlieff conducted data and image processing for the entire project. Author J. S. Reid provided key ideas and conducted extensive review/revisions of the study. Steve Miller provided the nighttime lunar model necessary to complete the study.

Competing interests

The authors declare that they have no conflict of interest.

605 Acknowledgements

The authors would like to thank the AERONET team for the AERONET data.

Financial support

This project was/is supported by NASA grants 80NSSC20K1748 and 80NSSC24K1180.

610



References

- Cao, C., Y. Bai, W. Wang, and T. Choi, 2019: Radiometric Inter-Consistency of VIIRS DNB on Suomi NPP and NOAA-20 from Observations of Reflected Lunar Lights over Deep Convective Clouds. *Remote Sensing*, **11**, 934, <https://doi.org/10.3390/rs11080934>.
- 615 Giles, D. M., Sinyuk, A., Sorokin, M. G., Schafer, J. S., Smirnov, A., Slutsker, I., Eck, T. F., Holben, B. N., Lewis, J. R., Campbell, J. R., Welton, E. J., Korkin, S. V., and Lyapustin, A. I.: Advancements in the Aerosol Robotic Network (AERONET) Version 3 database – automated near-real-time quality control algorithm with improved cloud screening for Sun photometer aerosol optical depth (AOD) measurements, *Atmos. Meas. Tech.*, **12**, 169–209, <https://doi.org/10.5194/amt-12-169-2019>, 2019.
- 620 Holben, B. N., Eck, T. F., Slutsker, I., Tanre, D., Buis, J. P., Setzer, A., Vermote, E., Reagan, J. A., Kaufman, Y. J., Nakajima, T., Lavenu, F., Jankowiak, I., and Smirnov, A.: AERONET – A federated instrument network and data archive for aerosol characterization, *Remote Sens. Environ.*, **66**, 1–16, 1998.
- Jackson, J. M., H. Liu, I. Laszlo, S. Kondragunta, L. A. Remer, J. Huang, and H.-C. Huang, 2013: Suomi-NPP VIIRS aerosol algorithms and data products. *Journal of Geophysical Research: Atmospheres*, **118**, 12,673–12,689, <https://doi.org/10.1002/2013JD020449>.
- 625 Johnson, R. S., J. Zhang, E. J. Hyer, S. D. Miller, and J. S. Reid, 2013: Preliminary investigations toward nighttime aerosol optical depth retrievals from the VIIRS Day/Night Band. *Atmospheric Measurement Techniques*, **6**, 1245–1255, <https://doi.org/10.5194/amt-6-1245-2013>.
- Knapp, K. R., T. H. Vonder Haar, Y. J. Kaufman: Aerosol optical depth retrieval from GOES-8: Uncertainty study and retrieval validation over South America. *Journal of Geophysical Research*, **107**, <https://doi.org/10.1029/2001JD000505>.
- 630 Kopp, T. J., W. Thomas, A. K. Heidinger, D. Botambekov, R. A. Frey, K. D. Hutchinson, B. D. Iisager, K. Brueske, B. Reed, 2014: The VIIRS Cloud Mask: Progress in the first year of S-NPP toward a common cloud detection scheme. *Journal of Geophysical Research: Atmospheres*, **119**, 2441–2456, <https://doi.org/10.1002/2013JD020458>.



- 635 Levy, R. C., S. Mattoo, L. A. Munchak, L. A. Remer, A. M. Sayer, F. Patadia, and N. C. Hsu, 2013: The Collection 6
MODIS aerosol products over land and ocean. *Atmospheric Measurement Techniques*, **6**, 2989–3034,
<https://doi.org/10.5194/amt-6-2989-2013>.
- Martins, J. V., D. Tanré, L. Remer, Y. Kaufman, S. Mattoo, and R. Levy, 2002: MODIS Cloud screening for remote sensing
of aerosols over oceans using spatial variability. *Geophysical Research Letters*, **29**, MOD4-1-MOD4-4,
640 <https://doi.org/10.1029/2001GL013252>.
- McHardy, T. M., J. Zhang, J. S. Reid, S. D. Miller, E. J. Hyer, and R. E. Kuehn, 2015: An improved method for retrieving
nighttime aerosol optical thickness from the VIIRS Day/Night Band. *Atmospheric Measurement Techniques*, **8**,
4773–4783, <https://doi.org/10.5194/amt-8-4773-2015>.
- Miller, S. D., and R. E. Turner, 2009: A Dynamic Lunar Spectral Irradiance Data Set for NPOESS/VIIRS Day/Night Band
645 Nighttime Environmental Applications. *IEEE Transactions on Geoscience and Remote Sensing*, **47**, 2316–2329,
<https://doi.org/10.1109/TGRS.2009.2012696>.
- Reid, J. S., Gumber, A., Zhang, J., Holz, R. E., Rubin, J. I., Xian, P., Smirnov, A., Eck, T. F., O’Neill, N. T., Levy, R. C.,
Reid, E. A., Colarco, P. R., Benedetti, A., & Tanaka, T. (2022). A Coupled Evaluation of Operational MODIS and
Model Aerosol Products for Maritime Environments Using Sun Photometry: Evaluation of the Fine and Coarse
650 Mode. *Remote Sensing*, *14*(13), 2978. <https://doi.org/10.3390/rs14132978>
- Remer, L. A., and Coauthors, 2005: The MODIS Aerosol Algorithm, Products, and Validation. *Journal of the Atmospheric
Sciences*, **62**, 947–973, <https://doi.org/10.1175/JAS3385.1>.
- Remer, L. A., S. Mattoo, R. C. Levy, and L. A. Munchak, 2013: MODIS 3 km aerosol product: algorithm and global
perspective. *Atmospheric Measurement Techniques*, **6**, 1829–1844, <https://doi.org/10.5194/amt-6-1829-2013>.
- 655 Ricchiazzi, P., S. Yang, C. Gautier, and D. Sowle, 1998: SBDART: A Research and Teaching Software Tool for Plane-
Parallel Radiative Transfer in the Earth’s Atmosphere. *Bulletin of the American Meteorological Society*, **79**, 2101–
2114, [https://doi.org/10.1175/1520-0477\(1998\)079<2101:SARATS>2.0.CO;2](https://doi.org/10.1175/1520-0477(1998)079<2101:SARATS>2.0.CO;2).
- Román, R., González, R., Toledano, C., Barreto, Á., Pérez-Ramírez, D., Benavent-Oltra, J. A., Olmo, F. J., Cachorro, V. E.,
Alados-Arboledas, L., and de Frutos, Á. M., 2020: Correction of a lunar-irradiance model for aerosol optical depth



- 660 retrieval and comparison with a star photometer, *Atmos. Meas. Tech.*, **13**, 6293–6310, <https://doi.org/10.5194/amt-13-6293-2020>.
- Shi, Y., Zhang, J., Reid, J. S., Holben, B., Hyer, E. J., and Curtis, C., 2018: An analysis of the collection 5 MODIS over-ocean aerosol optical depth product for its implication in aerosol assimilation, *Atmos. Chem. Phys.*, **11**, 557–565, <https://doi.org/10.5194/acp-11-557-2011>.
- 665 Vermote, E. F., D. Tanre, J. L. Deuze, M. Herman, and J.-J. Morcette, 1997: Second Simulation of the Satellite Signal in the Solar Spectrum, 6S: an overview. *IEEE Transactions on Geoscience and Remote Sensing*, **35**, 675–686, <https://doi.org/10.1109/36.581987>.
- Zhang, J., Reid, J. S., Turk, J., and Miller, S.: Strategy for studying nocturnal aerosol optical depth using artificial lights, *Int. J. Remote Sens.*, **29**, 4599–4613, 2008.
- 670 Zhang, J., J. S. Reid, B. T. Sorenson, S. D. Miller, M. O. Román, Z. Wang, R. J. D. Spurr, S. Jaker, T. F. Eck, and J. I. Rubin, 2019: Towards gridded nighttime aerosol optical thickness retrievals using VIIRS day–night band observations over regions with artificial light sources, *Atmos. Meas. Tech.*, **18**, 1787–1810, <https://doi.org/10.5194/amt-18-1787-2025>, 2025.
- Zhang, J., S. L. Jaker, J. S. Reid, S. D. Miller, J. Solbrig, and T. D. Toth, 2019: Characterization and application of artificial
675 light sources for nighttime aerosol optical depth retrievals using the Visible Infrared Imager Radiometer Suite Day/Night Band. *Atmospheric Measurement Techniques*, **12**, 3209–3222, <https://doi.org/10.5194/amt-12-3209-2019>.
- Zhou, M., J. Wang, X. Chen, X. Xu, P. Colarco, S. D. Miller, J. S. Reid, S. Kondragunta, D. M. Giles, and B. Holben, 2021: Nighttime Smoke Aerosol Optical Depth over U.S. Rural Areas: First Retrieval from VIIRS Moonlight
680 Observations. *Remote Sensing of Environment*, **267**, 112717, <https://doi.org/10.1155/2014/767231>.